Adjustable nanofabricated atomic size contacts

J. M. van Ruitenbeek
Kamerlingh Onnes Laboratorium, Leiden University, P.O. Box 9506, 2300 RA Leiden, The Netherlands

A. Alvarez, I. Piñeyro, and C. Grahmann
Departamento de Física, Facultad de Ciencias Físicas y Matemáticas, Universidad de Chile, Casilla 487-3, Santiago, Chile

P. Joyez, M. H. Devoret, D. Esteve, and C. Urbina
Service de Physique de l'Etat Condensé, CEA-Saclay, F-91191 Gif-sur-Yvette, France

(Received 26 July 1995; accepted for publication 2 October 1995)

Metallic point contacts and tunnel junctions with a small and adjustable number of conduction channels have been obtained in the last few years using scanning tunneling microscope and break junction techniques. For conventional break junctions, the reported drift of the interelectrode spacing in the tunnel regime is typically of the order of 0.5 pm/min (1 pm$=10^{-12}$ m). We have nanofabricated break junctions which display a drift smaller than 0.2 pm/h. The improvement results from the scaling down by two orders of magnitude of the device dimensions. We describe the nanofabrication process, which can be adapted to most metals. We have performed measurements on Al, Cu, and Nb devices. The results illustrate the ability of the technique to explore phenomenalike conductance quantization and two level fluctuations. These new adjustable atomic size contacts and tunnel junctions can be integrated in complex circuits. © *1996 American Institute of Physics.* [S0034-6748(96)02901-X]

I. INTRODUCTION

Electrical and mechanical properties of matter at the atomic level can now be investigated using the scanning tunneling microscope (STM) techniques. By pressing the tip of a STM against a metallic surface, point contacts of a few atoms have been made.[1–3] Recently, a related technique has been developed in which two metallic tips facing one another are fabricated *in situ* by breaking a thin wire clamped to an elastic substrate.[4] The method is an extension of the "break junction" technique pioneered by Moreland and co-workers.[5] Like in the STM experiments, the number of atoms forming the contact between the two electrodes can be mechanically adjusted one by one.[6] However, because the overall dimensions are smaller than those of a STM setup, these point contacts have by construction a much better interelectrode stability. Furthermore, they are easily implemented at low temperatures, at which atomic surface motions are frozen. A number of experiments have already taken advantage of this improved stability. When the contact consists of only a few atoms (with lateral dimensions lower than 3 nm) crystal lattice defects can be detected.[7] The size dependence of Kondo scattering has been investigated with these contacts.[8] In the tunneling regime the conductance stability of about 1%, corresponding to an electrode separation drift of 0.5 pm over a few minutes, has allowed the observation of multiparticle tunnel processes.[9]

The conventional mechanically controlled break junction setup is sketched in Fig. 1. A metallic wire, of diameter D, is attached to an elastic substrate (bending beam) of thickness t with two droplets of epoxy separated by a distance u. The wire is deeply notched with a knife in between the two epoxy anchors, thus forming a neck of diameter d and length l. The substrate is placed on two countersupports a distance L apart and bent by pushing in its center with a driving rod. The strain imposed on the suspended section of the wire by bending the beam is concentrated at the notch, by a factor $\epsilon=u/[l+(u-l)d^2/D^2]$. Typically, values of $\epsilon\approx 10$ can be achieved. Consequently, the wire can be broken before reaching the plastic deformation limit of the bending beam. After break, the electrodes can be brought back to contact. The contact area is then adjusted by controlling the bending of the beam with a piezoelectric actuator mounted in line with the driving rod. An elongation δx of the actuator translates into a stretch $\delta u=r\,\delta x$ of the suspended wire, where $r=6tu/L^2$ is the "displacement ratio" of the setup. This ratio determines the immunity of the system against external vibrations. Typical values for the substrate dimensions are $L=20$ mm and $t=1$ mm. The value of L is mainly limited by the available experimental room in a cryostat and t cannot be reduced significantly without prohibitive losses in rigidity. As the distance u between the epoxy anchors cannot be made in practice much smaller than 0.5 mm the displacement ratio is typically of the order of $r\approx 7\times 10^{-3}$.

We have developed a new technique which reduces the displacement ratio by at least two orders of magnitude. Using electron beam lithography we have fabricated metallic bridges with suspended lengths of the order of $u\approx 3$ μm. The technique also has the advantage that the neck geometry can be designed at will. The strain concentration factor ϵ can then be optimized and controlled in a reproducible way. We describe below the fabrication process and present experimental results that illustrate the operation of these devices.

II. FABRICATION PROCEDURE

The basic aim of the technique is to fabricate, from a thin metallic film deposited on an elastic substrate, a bridge suspended over a few micrometers.

 © 1996 American Institute of Physics

Downloaded¬17¬Sep¬2009¬to¬132.166.23.211.¬Redistribution¬subject¬to¬AIP¬license¬or¬copyright;¬see¬http://rsi.aip.org/rsi/copyright.jsp

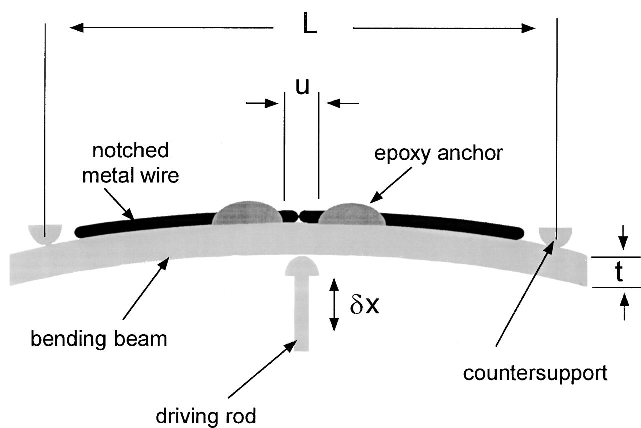

FIG. 1. Schematic drawing (not to scale) of the mechanically controllable break junction setup. A notched metallic wire is anchored at two points to a bending beam. The suspended section length is u, countersupports separation L, and substrate thickness t. When the driving rod bends the beam the suspended region elongates by $r\delta x$, where δx is the rod displacement and $r=6tu/L^2$ is the displacement ratio.

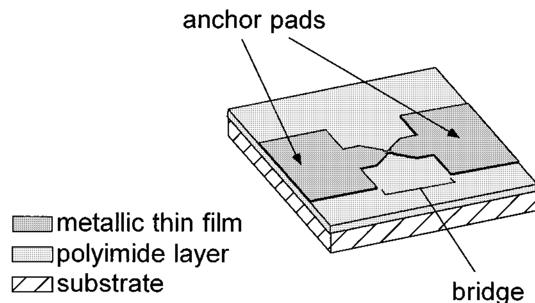

FIG. 2. Schematic view (different vertical and horizontal scales) of a sample after evaporation and lift-off of the metal thin film. The 3-μm-thick polyimide layer acts both as an insulating and planarizing layer. In the fabrication process, the selective removal of the polyimide layer under the central strip marked "bridge" frees it from the substrate. The large-area metallic regions remain anchored to the substrate. The neck in the bridge acts as a strain concentrator when bending the substrate. This neck can be as small as 100 nm wide and 100 nm long.

Although in principle any elastic substrate can be used, we have worked on phosphor–bronze sheets (thickness $t=0.8$ mm). Metallic substrates are compatible with fine electron beam lithography as they readily evacuate the charges. After a crude polishing of the substrate (residual roughness close to 1 μm), an insulating layer is spun on it. This layer plays three roles. First, it planarizes the substrate surface to a level compatible with the smallest dimension of the devices (100 nm). Second, it insulates the metallic thin films from the substrate. Finally, it can be carved to free the bridge. This layer must be elastic enough not to crack during the bending of the beam. We have used a 3 μm layer of polyimide PI 2610 from Dupont de Nemours. A special thermal treatment is necessary for the polyimide layer to retain its elastic properties at low temperatures: First, the substrate is placed for 30 min in an oven at 200 °C to remove the solvent. Then, it is heated up to 350 °C in a vacuum chamber under a pressure lower than 10^{-3} Pa. After 30 min the substrate is allowed to slowly cool down to room temperature.

We have used standard electron beam lithography. A bilayer electrosensitive mask consisting of a 500-nm-thick layer of PMMA-MAA followed by a 50-nm-thick layer of PMMA is spun on the substrate. At this point, the substrate is diced into 20 mm×5 mm pieces which are subsequently processed separately. The bilayer is exposed to the electron beam of a scanning electron microscopy (SEM), scanned according to the pattern shown in Fig. 2. After development, the bilayer provides a mask for the deposition by evaporation of a metallic film, typically 100 nm thick. We have evaporated so far only Al and Cu but the method should be applicable to any conducting material for which good films can be obtained by evaporation (the case of refractory metals like Nb is described below). A lift-off is then performed by soaking the substrate in acetone.

The polyimide layer is carved, so as to suspend the bridge, in a reactive ion etcher under the following rf plasma conditions: 50 sccm of O_2 and 1 sccm of SF_6 at a total pressure of 28 Pa, and a bias voltage of 50 V. The sample is held on an aluminum block at 200 °C. Under these conditions the polyimide is isotropically etched at a rate close to 1 μm/min. The vertical etching depth is monitored by means of an interferometer. Etching 1 μm vertically is enough to free from the substrate the metallic features having lateral dimensions lower than 2 μm. A SEM photograph of a resulting free suspended bridge is shown in Fig. 3.

The process is readily adapted to refractory metals like Nb that are preferably deposited by sputtering. The refractory metal layer is deposited on the whole substrate just after the planarization polyimide layer. All the electron beam lithography steps are then performed as before. Then, a 10–20-nm-thick overlayer of Al is evaporated through the mask on top of the Nb layer. After lift-off, this overlayer is used as a mask for the etching of both the Nb film (in a pure SF_6 plasma) and the polyimide layer. At this point the overlayer can be removed if necessary by wet etching.

When the metallic strips are freed from the substrate, internal stresses or stress gradients can lead to deformation or even breaking of the bridges. Deposition parameters, which are material and equipment dependent, have to be carefully chosen to avoid these problems. For example, the Ar pressure during sputtering of the Nb layer was chosen low

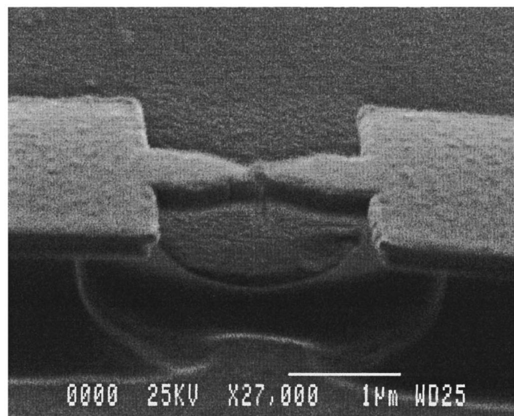

FIG. 3. Scanning electron microscope picture of a niobium device after operation. The Al overlayer was not removed. The polyimide layer has been carved underneath the smallest features by reactive ion etching. Although the narrow strip between the anchors is only 2 μm long, the length of the resulting suspended bridge is close to 3 μm due to the lateral etching.

Downloaded¬17¬Sep¬2009¬to¬132.166.23.211.¬Redistribution¬subject¬to¬AIP¬license¬or¬copyright;¬see¬http://rsi.aip.org/rsi/copyright.jsp

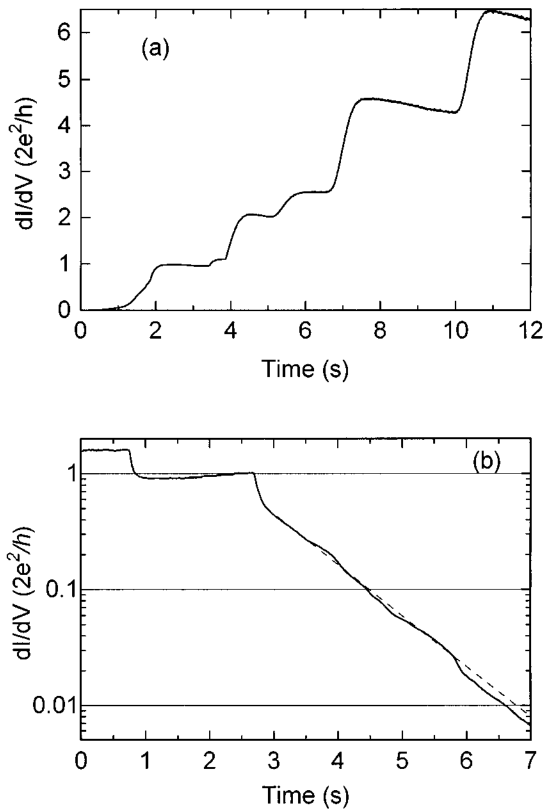

FIG. 4. (a) Conductance at $V=0$ of an Al device at 4.2 K when the two electrodes are driven into contact at a nominal rate of 17 pm/s. Jumps reveal different stable configurations of the contact involving only a few atoms. (b) Conductance of the same sample when the contact is broken at the same nominal rate. Note the logarithmic scale on the conductance axis. After the last conductance "plateau" the contact breaks and the conductance decreases exponentially with increasing interelectrode distance (tunneling regime). Deviations from smooth exponential behavior can be attributed to irregularities in the transmission of the driving mechanism. The dashed line is the best exponential decay fit giving a characteristic decay length for tunneling of 17 pm. The time constant of the measurement system was 0.1 s (panel a) and 0.3 s (panel b).

enough for the film to be under slight compression.

Finally, let us mention that a different nanoscale break junction fabrication process has been developed recently on Si substrates.[10]

III. EXPERIMENTAL RESULTS

Four terminal measurements are performed by connecting leads to large area pads using indium pellets. Ultrasound bonding proved to be very delicate and unreliable, probably due to the polyimide layer. The leads are filtered with simple *RC* filters.

The resistance of the bridge prior to deformation of the substrate is typically between 2 and 5 Ω although we have also found values up to 25 Ω. The chip is mounted on the countersupports ($L\approx 15$ mm) and cooled down to 4.2 K in a He atmosphere. A mechanical gear system, driven by a dc motor, pushes a rod against the elastic substrate playing the role of a bending beam. A gear box and a 0.8 mm pitch screw translate one turn of the motor into a 2 μm displacement of the rod. In turn, the nominal displacement ratio $r\approx 6.4\times 10^{-5}$ translates this displacement into a 130 pm stretching of the suspended bridge (we have taken $t\approx 0.8$ mm and $u\approx 3$ μm). The geometry of the suspended bridge can be designed to produce a strain concentration factor ϵ between 1 and 15, a wide enough range to reach the critical strains of most metals. For the geometry shown in Fig. 2, $\epsilon\cong 6$. The two freshly exposed electrodes, with a total area which can easily be as small as 100 nm×100 nm, are then brought back to contact using the same mechanical drive.

Figure 4(a) shows the conductance $dI/dV(V=0)$ of an Al device, as the two electrodes are brought back into contact from the tunnel regime at a nominal rate of 17 pm/s. The steps represent the making of the contact through successive atomic configurations involving only a few atoms. As found with the conventional technique, the conductance jumps are of the order of the conductance quantum $2e^2/h$, but no perfect quantization is observed. Each making of the contact on the same sample gives a different sequence of jumps. Nevertheless the first few steps are quite reproducible, pointing to the existence of well-defined stable atomic configurations.[11] Figure 4(b) shows the conductance of the same sample as the electrodes are pulled apart from contact at a nominal rate of 17 pm/s. After a last plateau at a conductance close to $2e^2/h$, the one atom contact breaks and the conductance varies exponentially with time. If we assume that the electrode spacing δ does increase at the nominal rate, we deduce a characteristic tunneling decay length of 17 pm. However, if we assume the relation

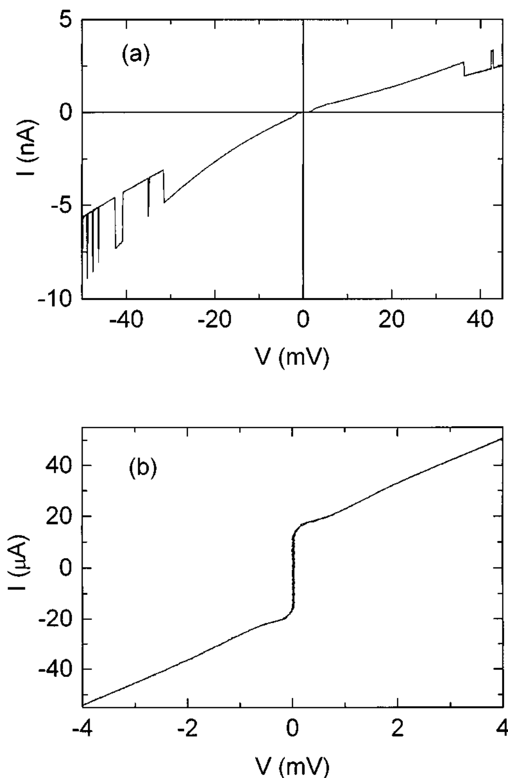

FIG. 5. Current–voltage characteristic of a Nb device at 4.2 K. (a) Tunnel regime ($R\geqslant 13$ kΩ). For this particular case $R\cong 15$ MΩ. The superconducting gap is visible in the central region. Due to thermal fluctuations no supercurrent is observed in this regime. Two-level fluctuations of conductance are induced by applied voltage above a threshold; (b) weak link regime ($R\leqslant 13$ kΩ). For this particular case $R\approx 115$ Ω. Note the supercurrent step at $V=0$.

Downloaded¬17¬Sep¬2009¬to¬132.166.23.211.¬Redistribution¬subject¬to¬AIP¬license¬or¬copyright;¬see¬http://rsi.aip.org/rsi/copyright.jsp

$dI/dV \propto \exp[-2(2m\phi)^{1/2}\delta/\hbar]$, where m is the free electron mass and $\phi \cong 4.2$ eV is the work function of Al, we expect a characteristic decay length of 47 pm. The discrepancy can arise for at least two reasons. First, we have used the work function value measured on a large surface. For two closely spaced small tips, the effective work function can be modified by screening effects.[12] Second, the displacement ratio r is calculated assuming an elastic deformation of the bending beam, which is not always the case in our present setup. In fact, despite the strain concentration ϵ imposed by design, breaking some of the samples required plastic deformation of the substrate, probably due to a compressive state of the deposited thin films. After the measurements these substrates clearly showed permanent deformation concentrated underneath the junctions.

We have found that it is possible to adjust a desired conductance even when manually driving the mechanical system. This illustrates the immunity of the design against external vibrations. The resistance of a device in the tunnel regime ($R \approx 4$ MΩ) drifted by no more than 5% in 16 h. If this drift is supposed to result from the sole variation of δ, the inferred interelectrode drift is no larger than 0.2 pm/h.

Figure 5(a) shows the current–voltage characteristics of a Nb device in the tunnel regime. The superconducting energy gap feature (of the order of 3 mV) is visible at the center of the characteristic. When voltages higher than 30–40 mV are applied across the junction, two-level fluctuations of the conductance are clearly visible. These fluctuations can arise either from motion of the forefront atoms on the electrodes induced by the current, or by the excitation of charge traps that could change the surface density of states. Figure 5(b) shows the current–voltage characteristic of a weak link obtained with the same sample in the contact regime ($R \approx 115$ Ω) and displaying a clear supercurrent branch.

To conclude, let us mention that the observed stability should allow inelastic electron tunneling spectroscopy of even a single molecule captured in the adjustable space between the electrodes. Also, these adjustable point contacts and tunnel junctions could be integrated in more complex circuits, e.g., like those of single electronics.[15] Finally, they provide a tool to investigate Josephson coupling between two superconductors in the case of a tunnel junction with a small number of conduction channels.

ACKNOWLEDGMENTS

This work has been partially supported by the Bureau National de la Métrologie and by Fondecyt (No. 19300938). One of us (C.U.) has benefited from grants from Fundación Andes (Programa de Profesores Visitantes C-12345/1) and Facultad de Ciencias Físicas y Matemáticas of Universidad de Chile where this work was started.

[1] N. Agraït, G. Rubio, and S. Vieira, Phys. Rev. Lett. **74**, 3995 (1995).
[2] L. Olesen, E. Lægsgaard, I. Stensgaard, F. Besenbacher, J. Schiotz, P. Stoltze, K. W. Jacobsen, and J. K. Norskov, Phys. Rev. Lett. **72**, 2251 (1994).
[3] J. I. Pascual, J. Méndez, J. Gómez-Herrero, A. M. Baró, N. García, and V. T. Binh, Phys. Rev. Lett. **71**, 1852 (1993).
[4] C. J. Muller, J. M. van Ruitenbeek, and L. J. de Jongh, Physica C **191**, 485 (1992).
[5] J. Moreland and J. W. Ekin, J. Appl. Phys. **58**, 3888 (1985).
[6] J. M. Krans, C. J. Muller, I. K. Yanson, Th. C. M. Govaert, R. Hesper, and J. M. van Ruitenbeek, Phys. Rev. B **48**, 14721 (1993).
[7] H. van Kempen and O. I. Shklyarevskii, Low Temp. Phys. **19**, 583 (1993).
[8] I. K. Yanson, V. V. Fisun, R. Hesper, A. V. Khotkevich, J. M. Krans, J. A. Mydosh, and J. M. van Ruitenbeek, Phys. Rev. Lett. **74**, 302 (1995).
[9] N. van der Post, E. T. Peters, I. K. Yanson, and J. M. van Ruitenbeek, Phys. Rev. Lett. **73**, 2611 (1994).
[10] C. Zhou, C. J. Muller, M. R. Deshpande, J. W. Sleight, and M. A. Reed, Appl. Phys. Lett. **67**, 1160 (1995).
[11] T. N. Todorov and A. P. Sutton, Phys. Rev. Lett. **70**, 2138 (1993).
[12] G. Binnig, N. García, H. Rohrer, J. M. Soler, and F. Flores, Phys. Rev. B **30**, 4816 (1984); N. Agraït, J. G. Rodrigo, and S. Vieira, Ultramicroscopy **42–44**, 177 (1992).
[13] For a review, see *Tunneling Spectroscopy*, edited by P. K. Hansma (Plenum, New York, 1982).
[14] G. Binnig, N. García, and H. Rohrer, Phys. Rev. B **32**, 1336 (1985).
[15] For a review, see *Single Charge Tunneling*, edited by H. Grabert and M. H. Devoret (Plenum, New York, 1992).

Downloaded¬17¬Sep¬2009¬to¬132.166.23.211.¬Redistribution¬subject¬to¬AIP¬license¬or¬copyright;¬see¬http://rsi.aip.org/rsi/copyright.jsp